

Diagenetic Evolution of Mudstones: Black Shales to Laminated Limestones, an Example from the Lower Jurassic of SW Britain

N. Arzani*

*Department of Geology, University of Payame-Nour, P.O. Box 81465-617,
Kohandej, Esfahan, Islamic Republic of Iran*

Abstract

The degree of carbonate cementation in argillaceous sediments represents one of the significant diagenetic evolutions in ancient mudstones. The alternation of the black shale and laminated limestone of the Lower Jurassic of SW Britain is an example, which typify extent of diagenetic modification of marine clay and organic-rich sediments. The Lower Jurassic mudstones of the SW Britain include black shales, marls and alternate with limestone beds and nodules. Laminated limestones are also present and are only enclosed between the black shales. Detailed petrography combined with geochemical analysis of the black shales and enclosed laminated limestones have been carried out and compared to the typical isolated nodules in order to interpret the diagenetic history of mudstones. Displacive growth of the microspar crystals was an important process that occurred during the diagenetic evolution of these mudstones. The black shales show carbon (+0.9 to +1.9‰ (PDB)) and oxygen (−2.2 to −4.1‰ (PDB)) isotopic values, which is compared to their enclosed laminated limestones, that show more negative carbon (−0.2 to −1.2 ‰ (PDB)) and oxygen (−5.4 to −6.8‰ (PDB)) values. The stratigraphic position, petrography and isotopic relationship of the black shales and enclosed laminated limestones indicate a degree of diagenetic evolution and carbonate cementation of mudstones during progressive burial.

Keywords: Diagenesis; Lower Jurassic; Black shale; Laminated limestone; mudstone

Introduction

Ancient mudstones have recorded significant diagenetic modification during their burial history. Carbonate cementation in the argillaceous sediments is one of these diagenetic processes whose origin has been much debated [5,7,25,29]. Early to late diagenetic

processes modify clay and organic-rich sediments to form distinctive authigenic mineral assemblages, among which carbonate cement is important to form limestone nodules to laterally extensive beds. The diagenetic evolution of the black shales to enclosed laminated limestones of the Lower Jurassic of SW Britain is an example, which shows the diagenetic modification of

* E-mail: arzan2@yahoo.com

marine, organic-rich, argillaceous sediments.

There is a voluminous literature about "depositional models", which have been proposed for the deposition of mudstones [18,24,36]. It is generally thought that black shales have been deposited in suboxic to anoxic environments and under fresh to estuarine to marine waters.

The early Jurassic, Lower Lias (Hettangian-Sinemurian) of south-west Britain consist of alternations of limestones-marls and black shales and typify epeiric sea, offshore sediments that altered largely by diagenesis [1,11,33]. In this sequence micritic limestones alternate with the marls and there are intervals dominated by marls or limestones. It has been argued that some micritic limestones in limestone-marl alternations could have been originated solely by diagenetic processes acting on an originally homogeneous sediment [6,12]. In other cases, it has been suggested that diagenesis has acted only to enhance primary sedimentological features [22,23,31,33].

Diagenetic models explaining the modification of rhythmically bedded marly and calcareous sequences have involved cementation processes controlled by the early decomposition of organic matter [2,28,29] or through differential cementation and dissolution processes [12,21]. This paper stresses the extent of diagenetic modification of argillaceous marine mudstones and their carbonate cementation to form laterally extensive limestone beds.

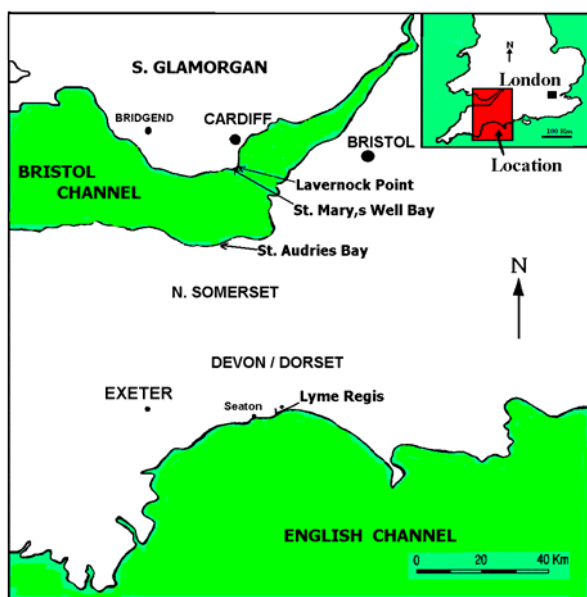


Figure 1. Location map, showing the position of the measured sections (arrowed) in SW Britain.

Geological Setting

The mudstone-limestone alternations of the Lower Lias are well exposed along the coastal sections of SW Britain (Glamorgan, Somerset & Dorset, Fig. 1) where they are gently dipping (Figs. 2 & 3). The Lower Lias (Pre-*planorbis* Beds to *bucklandi* Zone) belong to the Hettangian and lower Sinemurian and comprise up to 150 m of thinly interbedded limestones and marls/shales, a facies known as the Blue Lias. They represent offshore facies of a shallow sea that was part of an epeiric ocean (Northern Tethys) over NW Europe [13]. The open marine environment of the Lower Lias was established through a series of marine transgressive pulses that started in late Triassic [13]. This punctuated transgression was associated with the gradual inundation of the Carboniferous islands in south Glamorgan, where shallow marine nearshore facies of the Lias were deposited [1,16].

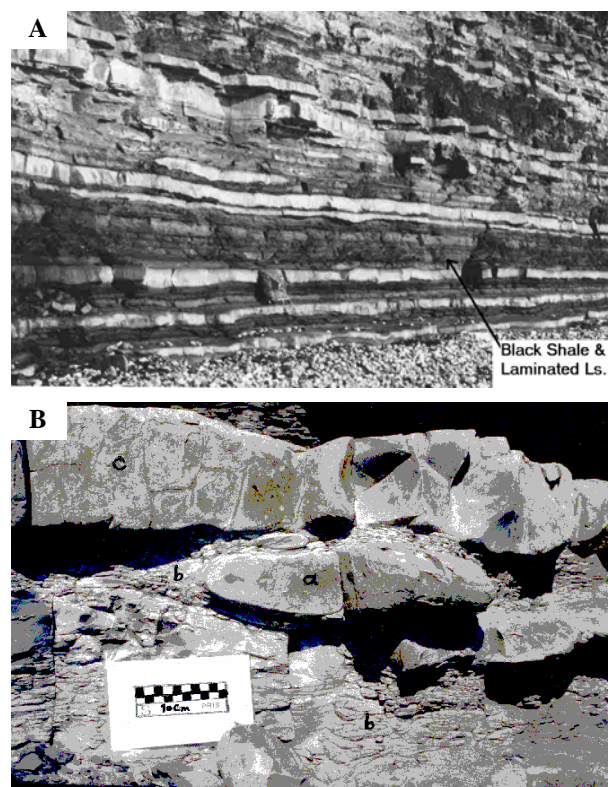


Figure 2. Field photographs (A & B) of the types of the lithologies typical of the Lower Lias. **A.** Part of *angulata* and *bucklandi* Zones (Hettangian-Sinemurian) in Lyme Regis, Dorset. Black shales and enclosed laminated limestones of the lower part of the section are arrowed. Rucksack for scale is 60 cm high. **B.** Part of *liasicus* Zone (Hettangian) in St Audries Bay, Somerset showing the isolated limestone nodules (a) between the marls (b). The laterally continuous limestone beds (nodular, c) are also shown.

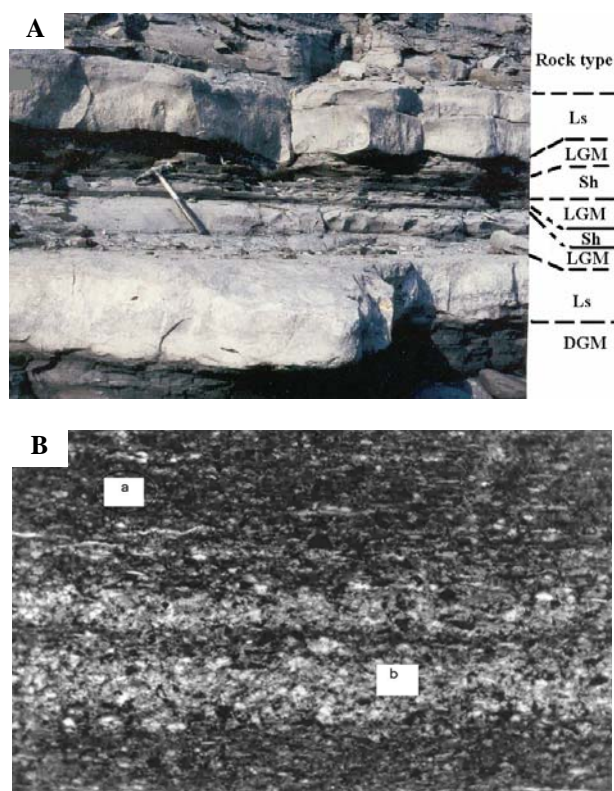


Figure 3. Field photograph (A) and thin section photomicrograph (B) of the Lower Lias black shale. A. Part of *angulata* Zone (Hettangian) of Lyme Regis, Dorset showing types of lithologies. Abbreviations are Ls= bioturbated limestone, LGM=light-grey marl, DGM=dark-grey marl and Sh= shale. B. Thin-section photomicrograph of the black shale, showing the clay-rich (a) and silt-rich (b) laminae. PPL and field of view 3 mm wide. Sample from *bucklandi* Zone, Somerset.

Methods

Normal and polished thin-sections of shale and laminated limestone were studied in transmitted light (48 sample), cathodoluminescence (CL) and by ultraviolet light microscopy (UV) (12 samples). The isolated limestone nodules, which were present between the marls, were cut into slabs and samples from edge and center of the nodules were studied.

Polished shale blocks of about 2 cm × 2 cm × 1 cm in size were prepared as epoxy-impregnated or embedded (4 sample). In order to minimize preparation damage caused by the presence of expanding clays, a non-aqueous cutting and polishing medium (paraffin) was used. Laminated limestone samples were cut into blocks of about 3 cm × 2 cm × 1 cm size (8 samples). The larger surface of each block was highly polished and slightly

etched following the method of [19] using 0.2% formic acid for 30 seconds. Following gold-coating, the surface of each block was examined under the SEM. The same surface was then repolished, coated with carbon and studied under the backscattered electron microscope (BSEM). During the BSEM examination of the carbon-coated samples, the BSEM was operated at 20 KV, 0.2 mA, and at a working distance of 8 mm. Fractured surface of samples was examined by SEM.

Carbon and oxygen stable isotope of the selected studied samples were prepared by drilling from polished surfaces, or by crushing and preparing powder samples from preselected rocks. The samples were analysed on a VGA SIRA Series II mass spectrometer following reaction with 100% phosphoric acid. Raw data were corrected following standard procedures and expressed as per mil variation from the PDB reference standards. Trace element compositions of powdered samples were determined by inductively coupled plasma atomic emission spectrometry (ICP). Acetic acid (10% v/v) was used for digestion of the carbonate fractions of the limestone and shale. Total organic carbon (TOC) of shale and laminated limestone has been determined using the wet titration method [9]. Degree of pyritization (DOP) has been measured using Raiswell's method [29]. All analysis performed in the Postgraduate Research Institute of Sedimentology, University of Reading, UK.

Field Observations

The Lower Lias black shales and laminated limestones of SW Britain comprise part of rhythmic alternations of limestones and marls/shales (Fig. 2). They have been classified into five facies: black shales, laminated limestones, dark-grey marls, light-grey marls and bioturbated limestones (Fig. 3A). Laminated limestones are enclosed within the black shales and nodular to bioturbated limestones occur between the marls [1,11,33].

Black Shale

The black shales, also known as dark, laminated shales [33], form thin (a few cm) to thick (up to 2 m) beds. They are blue-grey and fissile in weathered surfaces, but dark-grey to black and laminated (continuous for several meters) in fresh surfaces (Figs. 2 and 3). The lamination consists of clay- and organic matter-rich (up to 3 mm thick) and carbonate-rich (up to 0.6 mm thick) laminae. The silt-rich laminae (up to 0.7 mm thick) and rare shell laminae (up to a few mm thick) are also present. The fauna are composed of small shells

of bivalves (*Liostrea*, *Lima* and *Modiolus*), benthic foraminifers, ostracodes, compacted shells of ammonites and echinoderm and vertebrate fragments [1].

Laminated Limestone

The laminated limestones occur between the black shales and are common in the lower part of the sequence of the Lower Lias (Pre-*planorbis* Beds and *planorbis* Zone). This lithofacies comprises dark-grey limestone beds up to 35 cm thick (mostly about 10 cm) with planar surfaces between the black shales [11,34]. The laminae, which are obvious in the field or in the polished blocks, are laterally continuous (Fig. 4A). The sparse fauna within the limestones consists of ostracodes, rare ammonites, benthic foraminifers and vertebrate fragments.

Petrography

Black Shale

The black shales were laminated and composed of carbonate and clay-rich laminae (Fig. 3B). The carbonate-rich laminae were composed of clay and organic matter cemented by "non-ferroan calcite (micrite and microspar)", which were associated with abundant framboidal pyrite. The non-ferroan calcite of the laminated limestones were brightly luminescent (orange to weak brown) under cathodoluminescence microscope.

The clay-rich matrix of the rock showed flattened amorphous organic matter formed thin (up to 0.05 mm) and discontinuous laminae in the UV light examination of the uncovered thin sections. The organic laminae were laterally continuous for up to 5 mm. There was rare evidence of the presence of peloids with evident outline of the preserved organic matter.

BSEM examination of the surface of the polished blocks (resin embedded and normal blocks) showed the details of the clay-rich, carbonate-rich and silt laminae. The clay-rich laminae consisted of clay and organic-rich matrix with disseminated, isolated calcite crystals (3 to 50 μm in size), angular to subangular, detrital quartz grains, mica flakes, dolomite crystals, authigenic pyrite crystals (mostly less than 10 μm in size) and ostracode fragments (Fig. 5). The clay minerals and mica flakes were oriented parallel to the lamination. The large, isolated calcite crystals, which were irregular and elongated in shape, mostly displayed parallel alignments to the laminations. The carbonate-rich laminae consisted of calcite crystals (10-70 μm in size), which showed preferential orientation to the laminae (Fig. 5). These

calcite crystals either had cemented the fine silt laminae, or enclosed the dispersed, fine silt-sized (50-100 μm), detrital quartz grains. The area between the microspar crystals were filled with thin (a few microns), or thick (up to 20 μm) concentrations of clay, organic matter and framboidal pyrite crystals. The thickness of the cemented laminae varied from 150 to 400 μm . SEM examination of the fractured surface of this lithofacies showed that the clay minerals were not crystalline.

Laminated Limestone

Optical petrography of the laminated limestone samples showed that they consisted of three types of laminae. There were dominantly alternations of the carbonate-rich laminae with clay and organic-rich laminae, whereas the silt-rich laminae were also present (Fig. 4B). The clay and organic-rich laminae were up to 3 mm thick. These laminae contained abundant pyrite framboids, ostracode fragments and dispersed grains of silt-sized quartz, dolomite crystals and muscovite flakes. The carbonate-rich laminae composed of microspar crystals, which were non-ferroan in the stained thin sections.

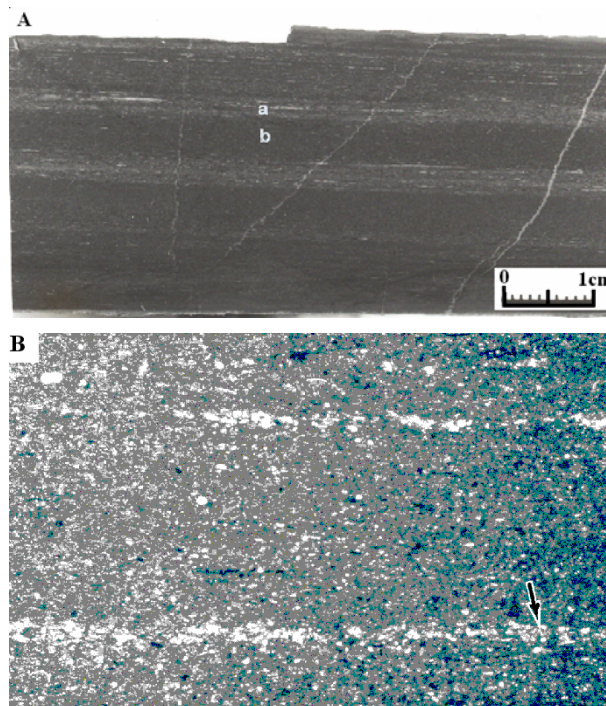


Figure 4. Polished hand specimen (A) and thin-section photomicrograph (B) of the Lower Lias laminated limestones. A. Alternations of the carbonate rich (a) and clay rich (b) laminae. B. Thin silt laminae (arrowed) in a carbonate-rich laminae. PPL and field of view is 1.2 mm. Sample from Pre-*planorbis* beds, Somerset.

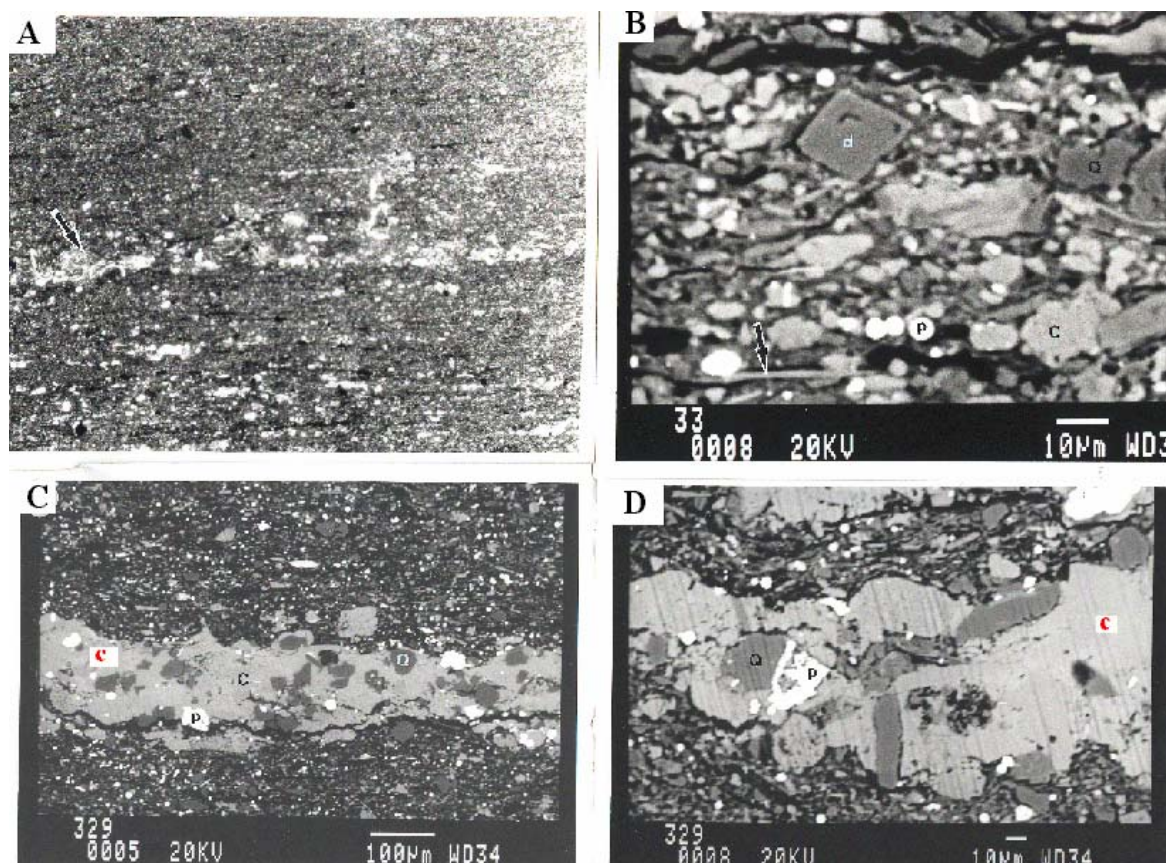


Figure 5. Thin section photomicrographs (A) and BSEM photomicrographs (B, C & D) of the surface of the polished blocks of the black shales of the Lower Lias. **A.** Thin silt laminae (arrowed) in the clay and organic-rich matrix. PPL and field of view 3 mm wide (sample from *bucklandi* Zone, Somerset). **B.** Part of a carbonate-rich laminae, showing the abundance of the microspar crystals (c), silt-sized quartz grains (Q), dolomite crystals (d), framboidal pyrite (p) and muscovite flakes (arrowed). Sample from 5 cm above the base of the Lower Lias, Pre-*planorbis* Beds, Lavernock Point, Somerset. **C & D.** Part of carbonate-rich lamina in clay and organic-rich matrix. Large microspar crystals (c) cementing the silt-sized quartz grains (Q). Sample from 6.2m above the base of Lower Lias, *planorbis* Zone, St. Audries Bay, Somerset.

SEM examination of the highly polished, etched surface of the laminated limestone blocks showed that the carbonate-rich laminae (up to 4 mm thick) consisted of microspar crystals up to about 20 μm (estimated mean about 8 μm) in diameter (Fig. 6). There were also small aggregates (up to 0.2 mm wide and about 30 μm thick) of microspar crystals (composed of unsorted crystals, about 6 to 20 μm in size) disseminated in the clay-rich laminae. These crystals were irregular, mostly elongated, with different orientations. The other components were clay flakes, pyrite crystals, silt-sized quartz grains and dolomite crystals. The silt-rich laminae (up to 0.4 mm thick and laterally continuous) were composed of corroded, fine, to medium silt-sized (up to 0.02 mm in diameter) quartz grains with disseminated crystals of dolomite, muscovite and ostracode fragments. There were also clay flakes

between the silt-sized quartz grains. These were cemented with non-ferroan calcite (microspar crystals, 6-20 μm in size and mean crystal size of 1.94 μm with an standard deviation of 0.89) (Fig. 6). Micrite crystals were subequant to mostly anhedral. They were partially surrounded by clay minerals, whereas the clay aggregates also formed a complete cage around few neighboring crystals. Clay flakes (inclusions) were present also within the calcite crystals. The intercrystalline boundary between the crystals were dominantly irregular (embayed interlocked grain contacts), however, rare straight to curvilinear crystal boundaries were also observable. There were few microspar crystals with enclosed submicron-sized, euhedral dolomite crystals. The silt-sized quartz grains and framboidal or single euhedral crystals of pyrite were also scattered in the micritic matrix.

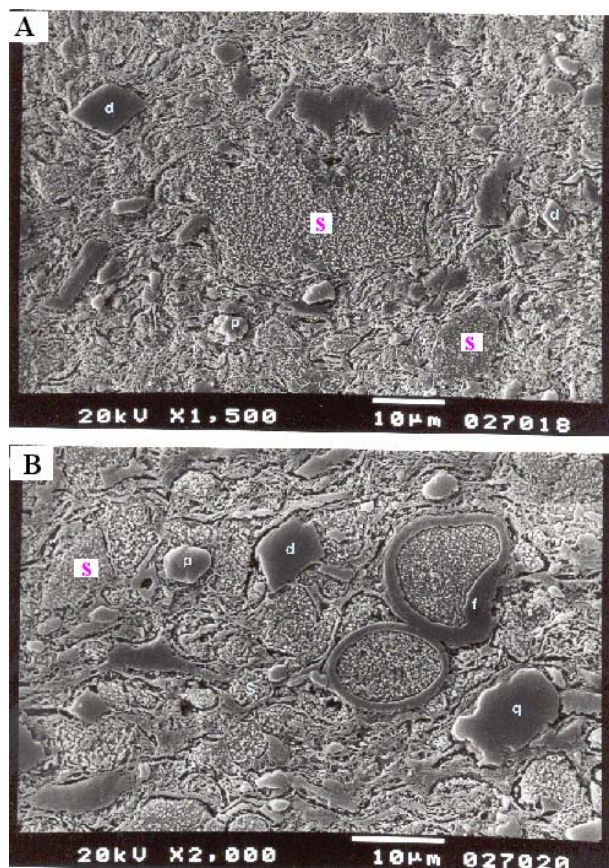


Figure 6. SEM photomicrographs (A & B) of the highly polished, etched surface of the Lower Lias laminated limestones (Pre-*planorbis* Beds, Somerset). Microspar crystals (s) floated in the clay matrix, framboidal pyrite (p), euhedral crystals of dolomite (d) and silt-sized quartz grains are present. Calcareous nannofossils (f) are also rarely present. Note the displacive growth of microspars with their clay inclusion (s). Sample DOB-2, Pre-*planorbis* Beds, Somerset (see text for explanation).

UV light examination showed that the compacted amorphous organic matter formed discontinuous laminae (up to 15 μm thick and laterally continuous for a maximum of 1.8 mm). There were also wood fragments dispersed in the fine clay matrix.

SEM examination of the fractured surface of this lithofacies showed rare presence of vague calcispheres or nano-planktons.

Geochemistry

Black Shale

The geochemical analyses of the selected samples of the black shales are presented in Table 1. The whole

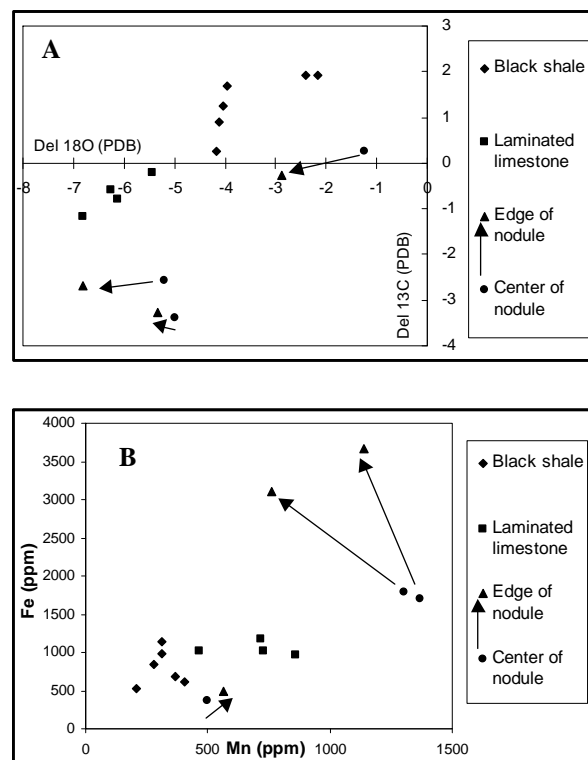


Figure 7. Cross plots of stable isotopic carbon & oxygen ratios (A) and ICP elemental analysis (Fe/Mn) (B) of the selected samples of the Lower Lias black shales and laminated limestones. The data of isolated limestone nodules are also shown for comparison. Arrows show trend from central to the edge of the corresponding nodule. **A.** The limestone-marl alternations of the Lower Lias have undergone a marine burial diagenesis, as there is no evidence of exposure to and development of fresh water regional aquifer below or above them (Arzani, 1997). The light $\delta^{18}\text{O}$ indicates that the formation of limestones has started at very shallow burial, but their cementation continued into deeper burial under more elevated temperature (see text for explanation). **B.** There is a weak trend in Fe/Mn ratios of shales to laminated limestones which is comparable to the nodule that its isotopic carbon is more close to shales. The other two limestone nodules, which are more negative in isotopic ratios (possibly later formed nodules), show a different trend (see Table 1).

rock analyses for stable carbon and oxygen isotopes of the black shales are plotted in Figures 7 and 8. The carbon and oxygen isotopic compositions of three distinct isolated limestone nodules of the Lower Lias of the measured section are also plotted in Figure 7A for comparison. The $\delta^{13}\text{C}$ values of the shales ranged from +0.90 to +1.92 per mil and $\delta^{18}\text{O}$ values were in the range of -2.17 to -4.12 per mil (PDB). Campos and Hallam [3] also reported isotopic ratios of a black shale sample from the Pre-*planorbis* Beds of Dorset ($\delta^{13}\text{C}$ of

Table 1. Geochemical (ICP, TOC, DOP and isotope) analysis of the black shales, laminated and nodular limestones of the Lower Lias of SW Britain

Sample No.	Description	AB* (cm)	CaCO ₃ (Wt %)	Mg (ppm)	Mn (ppm)	Al (ppm)	Fe (ppm)	Sr (ppm)	TOC (Wt%)	DOP	$\delta^{13}\text{C}$ (PDB)	$\delta^{18}\text{O}$ (PDB)
<i>Black shale</i>												
SB-1	Pre- <i>planorbis</i> Beds, St. Audries Bay, Somerset	10.0	18.2	15316	209	1118	533	628	4.80	0.87	1.92	-2.17
SB-4	Pre- <i>planorbis</i> Beds, St. Audries Bay, Somerset	165.0	20.0	13967	365	691	692	767	3.9	0.52	1.25	-4.04
SB-6	Pre- <i>planorbis</i> Beds, St. Audries Bay, Somerset	290	32.6	11447	279	1356	843	820	—	—	0.90	-4.12
SB-12	<i>Planorbis</i> Zones, St. Audries Bay, Somerset	680	34.0	6098	310	863	1146	321	—	—	0.26	-4.17
DOB-1	Pre- <i>planorbis</i> Beds, Doniford Bay, Somerset	5.0	21.4	10300	407	780	621	698	5.20	0.85	1.92	-2.41
DOB-3	Pre- <i>planorbis</i> Beds, Doniford Bay, Somerset	180.0	26.7	13781	312	1017	983	947	4.28	0.61	1.70	-3.95
PH-1	Pre- <i>planorbis</i> Beds, Dorset,	10.0	31.0	—	—	—	—	—	4.78	0.80	—	—
PH-2,	Pre- <i>planorbis</i> Beds, Dorset,	20.0	26.0	—	—	—	—	—	3.37	0.83	—	—
DGB-2	<i>bucklandi</i> Zone, Dorset,	1720	35.0	—	—	—	—	—	1.1	0.75	—	—
DGB-4	<i>bucklandi</i> Zone, Dorset,	1840	20.0	—	—	—	—	—	5.7	0.60	—	—
<i>Laminated limestone between the black shale and Isolated limestone nodule (edge & center of a single nodule) between the light marl</i>												
SB-3	Laminated limestone, Pre- <i>planorbis</i> Beds, St. Audries Bay, Somerset	150.0	76.3	7825	716	754	1174	564	—	—	-0.58	-6.27
DOB-2	Laminated limestone, Pre- <i>planorbis</i> Beds, Doniford Bay, Somerset	160.0	74.7	12420	467	547	1021	742	1.2	—	-0.22	-5.45
SBR-9a	Dark-grey laminae in a laminated limestone, Pre- <i>planorbis</i> Beds, Somerset	210.0	78.5	9269	861	664	958	426	0.9	—	-0.80	-6.12
SBR-9b	Light-grey laminae in a laminated limestone, Pre- <i>planorbis</i> Beds, Somerset	210.0	87.2	7762	726	565	1012	540	—	—	-1.17	-6.82
SBR-11E	Edge of a limestone nodule, <i>liasicus</i> Zone, St Audries Bay, Somerset	2380	68.3	13816	762	585	3104	529	—	—	-2.68	-6.81
SBR-12C	Center of a limestone nodule, <i>liasicus</i> Zone, St Audries Bay, Somerset	2380	81.8	9652	1301	525	1793	283	—	—	-2.56	-5.19
SLAV-1E	Edge of a limestone nodule, <i>liasicus</i> Zone, St Audries Bay, Somerset	2945	71	14314	1138	565	3663	309	—	—	-3.27	-5.34
SLAV-1C	Center of a limestone nodule, <i>liasicus</i> Zone, St Audries Bay, Somerset	2940	82.5	11597	1367	616	1705	260	—	—	-3.39	-5.00
PH-80E	Edge of a limestone nodule, <i>liasicus</i> Zone, Lyme Regis, Dorset	940	75	6098	566	533	492	372	—	—	-0.26	-2.89
PH-80C	Center of a limestone nodule, <i>liasicus</i> Zone, Lyme Regis, Dorset	935	84.5	7915	497	563	374	232	—	—	0.26	-1.52

Notes: (i) AB* = Distance above the base of the Blue Lias. (ii) Elemental values are normalised to 100% carbonate. (iii) ICP analyses were reproducible within 8% in all cases, and often within 2%. (iv) DOP values of < 0.75 are considered as normal oxygenated environments (Raiswell, *et al.*, 1988). See text for explanation.

+2.40‰ and $\delta^{18}\text{O}$ of -2.95‰), which is comparable to those of the studied Somerset samples. The elemental ratio of Fe/Mn is plotted in Figure 7B. Total organic carbon content (TOC) of the black shales varied in the

range of 1.1-5.7 wt%. Their carbonate content was variable between 18-56 wt%. The degree of pyritization (DOP) was between 0.52 to 0.87 (Table 1).

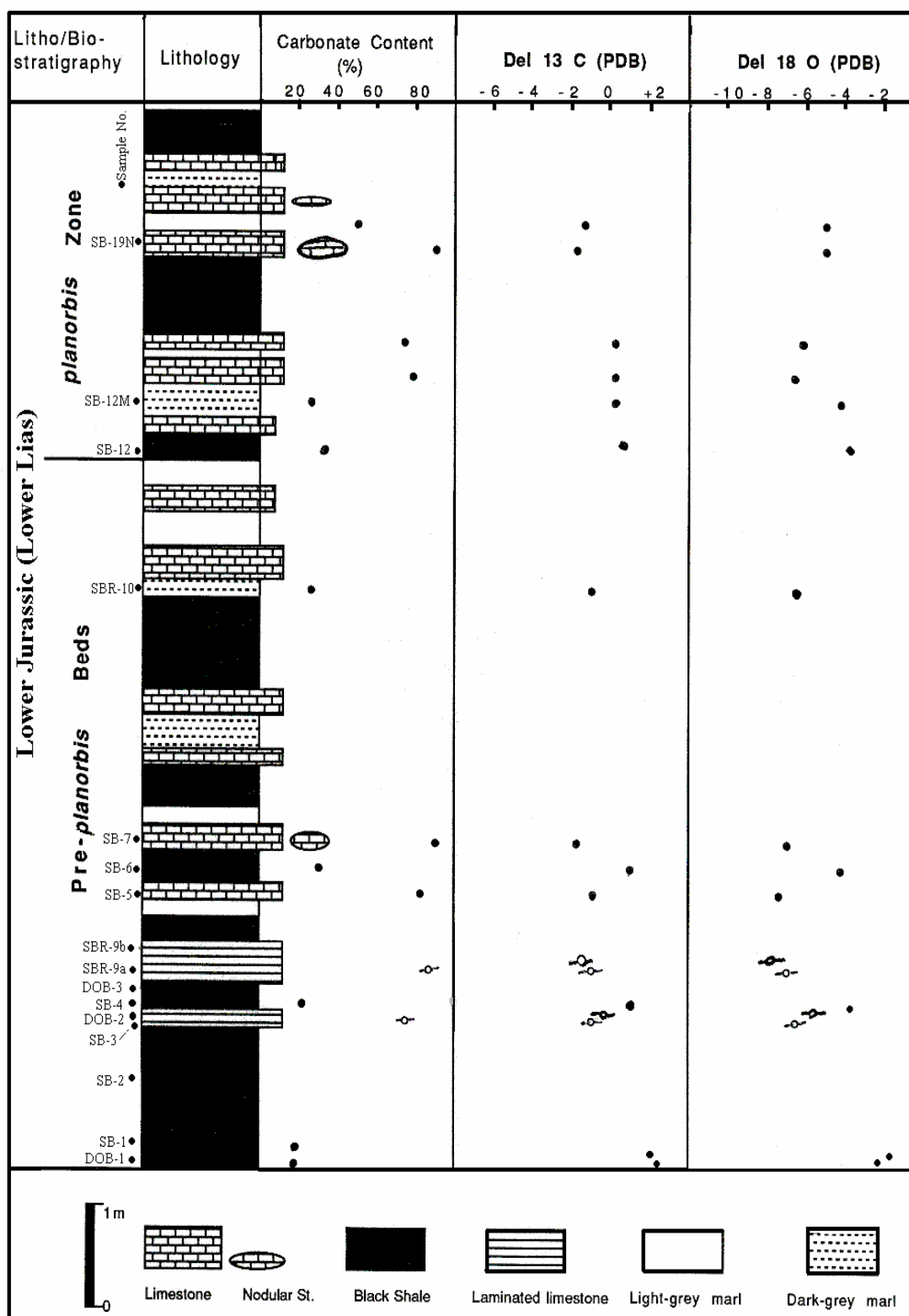


Figure 8. Sedimentological log with the plot of carbonate content and isotopic values (carbon & oxygen) of the lithologies of the basal part of the Lower Lias (Hettangian) in Somerset (see Figs. 2, 3 & 7 and the text for explanation).

Laminated Limestone

The geochemical analyses of the selected samples of the laminated limestones are presented in Table 1. The whole rock analyses for stable carbon and oxygen isotopes of laminated limestones are plotted in Figure 7A. The laminated limestones were slightly lighter in carbon isotopic values (-0.22 to -1.17 per mil), but lighter in oxygen values (-5.42 to -6.82 per mil) in comparison with the enclosed black shales. The elemental ratio of Fe/Mn is plotted in Figure 7B. The measured range of carbonate content of the selected samples from these laminated limestones was 68-82% (mean 75.8%) and total organic carbon varied from 1.2 to 3.3% (mean 1.7%) (Table 1).

Clay Mineralogy

XRD analysis of less than 2 μm clay mineral fractions of the black shales and laminated limestones showed that in both lithology the clay minerals were similar and illite was the dominant clay which comprised up to 80% of the total clay fraction. The other abundant clay minerals were mixed-layers, illite-smectite (expandable). Chlorite and kaolinite were the minor fraction of clay assemblages.

Discussion

Depositional and diagenetic models can be considered for the occurrence of the laminated limestone beds enclosed between the black shales. The alternations of the silt laminae with clay and organic-rich laminae of the black shales may indicate formation and preservation of depositional laminae [14,26,35]. The presence of the microspar laminae within the black shales represents diagenetic overprinting of this lithofacies.

Several depositional models have been proposed for the formation of black shales. The problem that the anoxia is caused by the over-abundance of organic matter (*productivity model*) or a failure of supply of benthic oxygen (*preservation model*) due to water column stratification is still controversial [8,24,25]. The laminated nature and DOP values (which measures the degree of bottom water oxygenation, Raiswell *et al.*, 1988) of the studied black shales indicate deposition under anoxic bottom water conditions.

The laminated limestones only occur between the black shales but not within marls or normal limestones of the Lower Lias sequence. The stratigraphic position of the laminated limestones combined with their petrography and geochemical indicate that the laminated

limestones probably formed by the cementation of the black shales. The presence of clay inclusions within the microspars of the laminated limestones indicates the displacive growth of the calcite cement. This is an important process that has occurred within the microspar laminae of the laminated limestones.

The laminated limestones are lighter in oxygen isotopic values (-5.42 to -6.82 per mil) compared with the enclosed black shales (Figs. 7A and 8). The $\delta^{13}\text{C}$ values of the black shales were within the range of reported average Jurassic marine cements (+2.75‰ (PDB) [15,32]. They are also comparable to those isotopic ratios from the calcitic shells of *Gryphaea* (8 samples) [34] from the limestone beds of the Lower Lias of Dorset ($\delta^{13}\text{C}$ of +1.6 to +1.78‰ and $\delta^{18}\text{O}$ of -0.37 to -0.84‰). The depletion of $\delta^{18}\text{O}$ of diagenetic carbonate is usually interpreted as the result of either precipitation at the higher temperature associated with burial, precipitation in equilibrium with isotopically light meteoric waters, or mixing with upward migrating basinal porewaters [17,27]. The possibility that meteoric waters invaded these offshore impermeable sediments during diagenesis is unlikely. The limestone-marl alternations of the Lower Lias have undergone a marine burial diagenesis, as there was no evidence of exposure and development of fresh water regional aquifer below or above them. The light $\delta^{18}\text{O}$ indicates that the formation of limestones started at very shallow burial, but their cementation continued into deeper burial under more elevated temperature. It has been suggested that progressive diagenesis through recrystallisation or additional cementation in subsurface waters would result in depletion with regard to ^{18}O [20]. The diagenetic trend of black shales to laminated limestones showed more primary carbonate in black shales toward more diagenetic carbonate in the laminated limestones, which was comparable to the diagenetic evolution of isolated limestone nodules (center to edge in Fig. 7). The black shales were cemented by non-ferroan calcite to form laminated limestones. The abundant framboidal pyrite and the non-ferroan nature of the microspars of the laminated limestones may indicate the importance of bacterial sulphate reduction in their formation. It has also been suggested that bacterial sulphate reduction [2,34] or anaerobic methane oxidation [28] were the main processes for the bicarbonate production during the formation of the limestones (beds and nodules) of the Lower Lias. Bottrell and Raiswell [2], based on the measurement of pyrite contents of the limestones and marls of the Lower Lias, suggested a prolonged mechanism of sulphate reduction for the formation of the Lower Lias limestones. Gluyas [10], based on $\delta^{13}\text{C}$ values of 16 samples (0.1 to -1.6‰) from nodular

limestones of the Lower Lias of Dorset, estimated that the bacterial sulphate reduction only provided 1% of the carbonate cement and the rest of cement was from a marine source. Although this ratio of cement from bacterial sulphate reduction may be an underestimation, however, it is probable that early dissolution (aragonitic bioclasts and carbonate mud) and reprecipitation of carbonate was an important source of carbonate for the lithification of the Lower Lias limestones [1].

Lamination within the shales may be produced through the compaction of benthic or planktonic faecal pellets and there is a great chance for the preservation of the faecal pellets in black shales due to the anoxic conditions, which minimize both biological and chemical degradation [4,26]. The variable thickness of the carbonate-rich laminae (changing laterally to as thin as two microspar crystal) and the absence of typical outline of the peloids in UV light may indicate that the microspar crystals comprising carbonate-rich laminae are not the result of peloids compaction.

The laminated limestones, which were stratigraphically developed between the black shales, were probably formed by the cementation of the black shales [1,33]. This shows the extent of diagenetic alteration (carbonate cementation) of argillaceous sediments, which may have implication for the understanding the diagenetic evolution of mudstones. However, the primary or diagenetic origin of limestones in limestone/mudstone alternations has been much debated [22,23,31,33].

Conclusions

1- The laminated limestones, which were stratigraphically developed between the black shales, were formed by the cementation of the black shales. This shows the extent of diagenetic alteration (carbonate cementation) of argillaceous sediments.

2- Early to late diagenetic processes modify clay and organic-rich sediments to form distinctive authigenic mineral assemblages, among which carbonate cementation is an important process to form limestone nodules to laterally extensive beds. Displacive growth of microspars and formation of carbonate-rich laminae within the clay matrix of the Lower Lias shale is an important process to form laminated limestones.

3- The carbon and oxygen isotopic compositions of the Lower Lias black shales and laminated limestones and their comparison with those of isolated limestone nodules indicate that the laminated limestones has been formed through the cementation of their enclosed black shales. The isotopic results neither show typical negative carbon values of the bacterial sulphate

reduction, nor the positive values of the methanogenesis, suggesting that the bicarbonate was mainly sourced through dissolution of marine carbonate.

References

1. Arzani N. Facies and Diagenesis at the Triassic-Jurassic boundary in SW Britain. Ph.D. Thesis, University of Reading, UK, 381 p. (1997).
2. Bottrell S. and Raiswell R. Primary versus diagenetic origin of Blue Lias rhythms (Dorset, UK.): evidence from sulphur geochemistry. *Terra Nova*, **1**: 451-456 (1989).
3. Campos H.S. and Hallam A. Diagenesis of English Lower Jurassic limestones as inferred from oxygen and carbon isotope analysis. *Earth and Planetary Science Letters*, **45**: 23-31 (1979).
4. Cuomo M.C. and Bartholomew P.R. Pelletal black shale: their origin and significance. In: Tyson R.V. and Pearson T.H. (Eds.), *Modern and Ancient Continental Shelf Anoxia: an overview*. Geological Society Special Publication, No. 58: 221-232 (1991).
5. Curtis C.D. Post-depositional evolution of mudstones 1: early days and parental influences. *Journal of Geological Society, London*, **152**: 577-586 (1995).
6. Eder W. Diagenetic redistribution of carbonate, a process in forming limestone-marl alternations (Devonian and Carboniferous, Rheinisches Schiefergebirge, W. Germany). In: Einsele G., Ricken W., and Seilacher A. (Eds.), *Cycles and Events in Stratigraphy*. Springer-Verlag, Berlin, pp. 98-112 (1982).
7. El Albani A., Cloutier R., and Candilier A.M. Early diagenesis of the Upper Devonian Escuminac Formation in the Gaspé Peninsula, Québec: sedimentological and geochemical evidence. *Sedimentary Geology*, **146**(3-4): 209-223 (2002).
8. Filippelli G.M., Sierro G.M.F., Flores J.A., Vázquez A.V., Utrilla R., Pérez-Folgado M., and Latimer J.C. A sediment-nutrient-oxygen feedback responsible for productivity variations in Late Miocene sapropel sequences of the western Mediterranean. *Palaeogeography, Palaeoclimatology, Palaeoecology*, **190**: 335-348 (2003).
9. Gaudette H.E. and Flight W.R. An inexpensive titration method for the determination of organic carbon in recent sediments. *Journal of Sedimentary Petrology*, **44**: 249-253 (1974).
10. Gluyas J.G. The genesis and diagenesis of shale nodular limestone sequences. Unpublished Ph.D. Thesis, University of Liverpool (1983).
11. Hallam A. A sedimentary and faunal study of the Blue Lias of Dorset and Glamorgan: Philosophical Transactions of the Royal Society of London, B, No. 698, **243**: 1-44 (1960).
12. Hallam A. Origin of minor limestone-shale cycles: climatically induced or diagenetic? *Geology*, **14**: 609-612 (1986).
13. Hallam A. Estimation of the amount and rate of sea-level change across the Rhaetian-Hettangian and Pliensbachian-Toarcian boundaries (latest Triassic to early Jurassic). *Journal of geological Society London*, **154**: 773-779 (1997).
14. Herrle J.O., Pross J., Friedrich O., Koszler P., and

- Hemleben C. Forcing mechanisms for mid-Cretaceous black shale formation: evidence from the Upper Aptian and Lower Albian of the Vercors basin (SE France). *Palaeogeography, Palaeoclimatology, Palaeoecology*, **190**: 399-426 (2003).
15. Jenkyns H.C. and Clayton C.J. Black shales and carbon isotopes in pelagic sediments from the Tethyan Lower Jurassic. *Sedimentology*, **33**: 87-106 (1986).
 16. Johnson M.E. and MacKerrow W.S. The Sutton Stone: an early Jurassic rocky shore deposit in South Wales. *Palaeontology*, **38**(3): 529-541 (1995).
 17. Land L.S. The carbon and oxygen isotopic chemistry of surficial shallow marine carbonate sediment and Quaternary limestone and dolomite. In: Fritz P. and Fontes J.Ch. (Eds.), *Handbook of Environmental Isotopic Geochemistry*. Elsevier, 428 pp. (1989).
 18. Langrock U., Stein R., Lipinski M., and Brumsack H. Late Jurassic to Early Cretaceous black shale formation and paleoenvironment in high northern latitudes: Examples from the Norwegian-Greenland Seaway. *Palaeogeography*, **18**(3): 1074 (2003).
 19. Lasemi Z. and Sandberg P. Transformation of aragonite-dominated lime muds to microcrystalline limestones. *Geology*, **12**: 420-423 (1984).
 20. Moshier S.O. Microporosity in micritic limestones: a review. *Sedimentary Geology*, **63**: 191-213 (1989).
 21. Munnecke A. and Samtleben C.K. The formation of micritic limestones and the development of limestone-marl alternations in the Silurian of Gotland, Sweden. *Facies*, **34**: 159-176 (1996).
 22. Munnecke A. and Westphal H. Shallow-water aragonite recorded in bundles of limestone-marl alternations-the Upper Jurassic of SW Germany. *Sedimentary Geology*, **164**(3-4): 191-202 (2003).
 23. Munnecke A., Westphal H., Elrick M., and Reijmer J.J.G. The mineralogical composition of precursor sediments of calcareous rhythmites: a new approach. *International Journal of Earth Sciences*, **90**: 795-812 (2001).
 24. Negri A., Cobianchi M., Luciani V., Fraboni R., Milani A., Claps M. Tethyan Cenomanian pelagic rhythmic sedimentation and Pleistocene Mediterranean sapropels: is the biotic signal comparable? *Palaeogeography, Palaeoclimatology, Palaeoecology*, **190**: 373-397 (2003).
 25. O'Brien N.R. Shale lamination and sedimentary processes. In: Kemp A.E.S. (Ed.), *Palaeoclimatology and Palaeoceanography from Laminated Sediments*. Geological Society Special Publication No. 116: 23-36 (1996).
 26. O'Brien N.R. and Slatt R.M. *Argillaceous Rock Atlas*. Springer, 141pp. (1990).
 27. Qing H., Bosence D.W.J., and Rose E.P.F. Dolomitization by penesaline sea water in Early Jurassic peritidal platform carbonates, Gibraltar, western Mediterranean. *Sedimentology*, **48**(1): 153-168 (2001).
 28. Raiswell R. Non-steady state microbiological diagenesis and the origin of concretions and nodular limestones. In: Marshall J.D. (Ed.): *Diagenesis of Sedimentary Sequences*. Geological Society, London, Special Publication, No. 36: 41-54 (1987).
 29. Raiswell R. Chemical model for the origin of minor limestone-shale cycles by anaerobic methane oxidation. *Geology*, **16**: 641-644 (1988).
 30. Raiswell R., Buckley F., Berber R.A., and Anderson T.F. Degree of pyritization of iron as a palaeoenvironmental indicator of bottom-water oxygenation. *Journal of Sedimentary Petrology*, **58**(5): 812-819 (1988).
 31. Ricken W. Bedding rhythms and cyclic sequences as documented in organic carbon-carbonate patterns, Upper Cretaceous, Western Interior, U.S. *Sedimentary Geology*, **102**: 131-154 (1996).
 32. Romanek C.S., Grossman E.L., and Morse J.W. Carbon isotopic fractionation in synthetic aragonite and calcite: effects of temperature and precipitation rate. *Geochimica et Cosmochimica Acta*, **56**: 419-430 (1992).
 33. Weedon G.P. Hemipelagic shelf sedimentation and climatic cycles, the basal Jurassic (Blue Lias) of South Britain. *Earth and Planetary Science Letters*, **76**: 321-335 (1986).
 34. Weedon G.P. Paleoclimatic significance of open marine sequences. Ph.D. Thesis, University of Oxford, UK (1987).
 35. Wetzel A. Stratification in black shales: deposition models and timing- an overview. In: Einsele G., Ricken W., and Seilacher A. (Eds.), *Cycles and Events in Stratigraphy*. Springer-Verlag, Berlin, 955 pp. (1991).
 36. Wignall P.B. and Hallam A. Biofacies, stratigraphic distribution and depositional models of British onshore Jurassic black shales. In: Tyson R.V. and Pearson T.H. (Eds.), *Modern and Ancient Continental Shelf Anoxia*. Geological Society Publication, No.58: 291-309 (1991).